Transplantation of skeletal myoblasts secreting an IL-1 inhibitor modulates adverse remodeling in infarcted murine myocardium

Bari Murtuza*†, Ken Suzuki*, George Bou-Gharios†, Jonathan R. Beauchamp†, Ryszard T. Smolenski*, Terence A. Partridge†, and Magdi H. Yacoub*‡

*Cell and Gene Therapy Group, National Heart and Lung Institute, Imperial College Faculty of Medicine, London UB9 6JH, United Kingdom; and †Muscle Cell Biology Group, Medical Research Council Clinical Sciences Centre, Imperial College Faculty of Medicine, London W12 ONN, United Kingdom

Edited by Eugene Braunwald, Brigham and Women's Hospital, Boston, MA, and approved January 2, 2004 (received for review September 25, 2003)

After myocardial infarction (MI), adverse remodeling with left ventricular (LV) dilatation is a major determinant of poor outcome. Skeletal myoblast (SkM) implantation improves cardiac function post-MI, although the mechanism is unclear. IL-1 influences post-MI hypertrophy and collagen turnover and is implicated in SkM death after grafting. We hypothesized that SkM expressing secretory IL-1 receptor antagonist (sIL-1ra) at MI border zones would specifically attenuate adverse remodeling and exhibit improved graft cell number. Stable murine male SkM lines (5×10^5 cells), expressing or nonexpressing (cont) for sIL-1ra, were implanted into infarct border zones of female nude mice immediately after left coronary artery occlusion. LV ejection fraction (LVEF), end-diastolic diameter, and transmitral peak early/late (E/A) flow velocity ratio were determined by echocardiography. Cardiac myocyte hypertrophy and fibrosis were assessed by morphometry, picrosirius red staining, and hydroxyproline assay. At 3 weeks, cont-SkM-engrafted hearts showed reduced hypertrophy, improved LVEF (55.7 ± 1.2% vs. MI-only: 40.3 ± 2.9%), and preserved E/A ratios. sIL-1ra-SkM implantation enhanced these effects (LVEF, 67.0 ± 2.3%) and significantly attenuated LV dilatation (LV end-diastolic diameter, 4.0 ± 1.1 mm vs. cont-SkM, 4.5 ± 1.2 mm vs. MI-only, 4.8 ± 1.8 mm); this was associated with greater graft numbers, as shown by PCR for male-specific *smcy* gene. Enzyme zymography showed attenuated matrix metalloproteinase-2 and -9 up-regulation post-MI by either donor SkM type, although infarct-remote zone collagen was reduced only with sIL-1ra-SkM. These results suggest that SkM implantation improves cardiac function post-MI by modulation of adverse remodeling, and that this effect can be significantly enhanced by targeting IL-1 as a key upstream regulator of both adverse remodeling and graft cell death.

Transplantation of skeletal myoblasts (SkM) to the infarcted heart has consistently been shown to improve cardiac function in experimental models of heart failure (1, 2). SkM survive, proliferate, and differentiate within the myocardium (3), although the mechanism of the consequent functional effects is unclear. It has been suggested that cell transplantation can modulate remodeling of the infarcted heart and, further, that implanted SkM may exert important paracrine effects on the surrounding host myocardium (1, 4).

Adverse remodeling after myocardial infarction (MI) can have a significant impact on global cardiac function and progression to chronic heart failure (5, 6). After MI, cardiac myocyte death and wall thinning lead to a complex cascade of remodeling events resulting in cardiac myocyte hypertrophy and apoptosis and a net increase in extracellular matrix (ECM) accumulation within the noninfarcted myocardium (7, 8). The exact mechanism of remodeling is unclear, although an important role has been proposed for cytokines (8–11).

IL-1 is a key paracrine mediator of adverse post-MI remodeling, which is also implicated in SkM death after grafting to muscle (8, 12). IL-1 induces hypertrophy of cardiac myocytes *in vitro*, and inhibition of IL-1 attenuates acute inflammation and cardiac myocyte apoptosis after ischemia-reperfusion injury in rat hearts (10, 13). Further, IL-1 expression correlates with left ventricular (LV) collagen content and LV end-diastolic diameter (LVEDD) after MI in rats and induces collagen gene transcription in fibroblasts (8, 14). Matrix metalloproteinase (MMP) types 2 and 9 (MMP-2/-9) are key gelatinases shown to be directly involved in post-MI ECM turnover (15). IL-1 stimulates expression of MMP-2 in ischemic cardiac fibroblasts and is a regulator of MMP-9 (16, 17). No studies, however, have exploited sustained IL-1 inhibition as a means to target adverse post-MI remodeling.

In addition to a role in myocardial remodeling, elevated IL-1 levels within the myocardium in the vicinity of implanted SkM are likely to be an important determinant of graft size (12). Rapid attrition of graft size is currently a major limitation to the efficacy of cell transplantation after direct intramyocardial implantation (18). Although this technique allows selective delivery to either infarcted or noninfarcted areas, it inevitably results in mechanical injury and acute inflammation (19). IL-1 is a major proinflammatory cytokine that induces apoptosis of primary human SkM *in vitro* (20) and has been suggested to be important in SkM survival *in vivo* (12).

The effects of IL-1 are balanced by an endogenous inhibitor, IL-1 receptor antagonist (IL-1ra). IL-1ra is part of the IL-1 gene cluster on chromosome 2 and exists as several variants generated by alternative splicing (21). Of these, the 17-kDa secretory IL-1ra isoform (sIL-1ra) appears to mediate the biological inhibitory effects of IL-1ra by competing for IL-1 receptor type I (21). We hypothesized that SkM modified to express sIL-1ra would exhibit an enhanced ability to modulate adverse remodeling after transplantation to the infarcted heart through effects on cardiac myocyte hypertrophy, ECM matrix turnover, and graft cell loss.

Materials and Methods

Generation of *H-2K*^{b}-sIL-1ra SkM Lines. SkM lines were derived from male *H-2K*^{b}-tsA58 mice as before (22). SkM were grown under permissive conditions at 33°C, 10% CO_2 in DMEM (GIBCO) growth medium with 20 units/ml IFN-γ (ICN). cDNA for human sIL-1ra was cloned by PCR into pcDNA3.1$^+$ (Invitrogen), as done previously (10). SkM were transfected by using FuGENE6 (Roche Diagnostics) and linearized (*Bgl*II) pcDNA3.1$^+$-sIL-1ra construct or control pcDNA3.1$^+$ plasmid. G418-resistant clones were obtained by limiting dilution and expanded for 5 weeks.

This paper was submitted directly (Track II) to the PNAS office.

Abbreviations: SkM, skeletal myoblast; IL-1ra, IL-1 receptor antagonist; sIL-1ra, secretory IL-1ra; ECM, extracellular matrix; MI, myocardial infarction; LV, left ventricular; LVEDD, LV end-diastolic diameter; MMP, matrix metalloproteinase; MMP-2/-9, MMP type 2/9; TGF, transforming growth factor; cont, nonexpressing for sIL-1ra.

‡To whom correspondence should be addressed. E-mail: b.murtuza@imperial.ac.uk.

www.pnas.org/cgi/doi/10.1073/pnas.0306205101

Cell supernatants from known SkM numbers were used for sIL-1ra enzyme immunoassay by using a kit and specified instructions (BioSource International, Camarillo, CA) and secretion rates expressed as pg per million cells per 24 h. Immunoctyochemistry was performed on SkM lines according to the method of Springer *et al.* (23) by using a monoclonal human-specific sIL-1ra antibody (R & D Systems). Differentiation into myotubes was induced by switching clones to nonpermissive conditions of low-serum, 37°C, and no IFN-γ (22).

Experimental Protocol, Surgery, and Animal Care. Left coronary artery occlusion was performed in female BALB/c-nu/nu mice (7–10 weeks; Harlan Breeders, Oxon, U.K.) under mechanical ventilation (24) and anesthesia with s.c. ketamine (0.1 mg/g) and xylazine (0.005 mg/g). Three experimental groups were used: MI plus sIL-1ra-SkM ($n = 26$), MI plus cont-SkM ($n = 27$) (cont, nonexpressing for sIL-1ra), and MI-only ($n = 25$). SkM were implanted at the time of coronary artery ligation: 0.25 million (in 5 μl of serum-free DMEM) into each of the two infarct border zones. All samples were analyzed at 3 weeks, and additional samples at 1 week were obtained for *smcy* PCR and matrix metalloproteinase zymography. This study was performed with approval of the institutional ethics and gene manipulation committees and the Government Home Office, London, U.K. This work conforms to the Principles of Laboratory Animal Care, National Society for Medical Research, and the Guide for the Care and Use of Laboratory Animals (National Institutes of Health Publication No. 85-23).

Assessment of LV Function and Size. Mice were anesthetized with s.c. ketamine and xylazine (25) at one-third the surgical dose and echocardiography performed by two blinded skilled operators by using a Sequoia 512 system and 15 MHz probe (Acuson, Mountain View, CA). All images were taken at the midpapillary level. Ejection fraction was calculated as described (25). Measurements of LVEDD were obtained from M-mode images. As an index of LV diastolic function, transmitral E/A values were determined from five measurements of each individual experimental subject (total of $n = 5$ for each group) by using spectral Doppler traces as described by Li *et al.* (9).

***smcy* PCR and sIL-1ra RT-PCR.** RNase-treated genomic DNA was phenol/chloroform-extracted from LVs (LV free wall plus interventricular septum) harvested at 1 and 3 weeks, as described (26). For standard curve samples, known numbers of male SkM (0.01–1.5 million) were mixed with female hearts. Five hundred nanograms of DNA was used in PCR with *smcy* primers (27) or *hprt* as a control (see sequences in Table 2, which is published as supporting information on the PNAS web site). The thermocycle profile used for *smcy* was: 94°C, 3 min; 40 cycles of 55°C, 1 min; 72°C, 1 min; 94°C, 30 sec, followed by final steps of 55°C, 1 min and 72°C, 10 min. PCR products (10 μl) were run on a 2% agarose gel, stained with ethidium bromide, and visualized with a UV transilluminator (Bio-Rad). Values for intensity of *smcy* bands were obtained by using NIH IMAGE analysis software and plotted against known SkM number to generate the standard curve from which SkM numbers for the experimental samples were calculated. Results for the yield of donor cell-derived *smcy* genomes in cell-engrafted hearts were expressed as percentages of the signal obtained for the originally implanted cell number (0.5×10^6). For IL-1ra RT-PCR, we used 1 μg of cDNA (prepared as below) and primer sequences/conditions for human or murine isoforms (Table 2).

Histological Identification of Implanted SkM. Harvested hearts were cut into five segments parallel to the apex-base axis. Segments were embedded in OCT compound (Tissue-Tek, BDH) and frozen in isopentane cooled in liquid nitrogen. Ten-micrometer cryosections were fixed in 4% paraformaldehyde. Endogenous peroxidase activity was quenched with 0.3% H_2O_2 and blocking performed as before (28). Sections were then stained by using a three-layer immunoperoxidase (horseradish peroxidase) technique with a skeletal muscle fast myosin-specific primary antibody (clone MY-32, Sigma), as described (24). Sections were counterstained with methyl green.

Infarct Size and Histological Analysis of Cardiac Myocytes and ECM. Ten-micrometer cryosections were cut, fixed in 10% neutral-buffered formal-saline, and stained with 0.1% picrosirius red F3B (BDH), as described by Ducharme *et al.* (15). Picrosirius red-stained sections from individual segments were imaged by using a computer-associated light microscope (Zeiss) and infarct size determined by planimetry by using NIH IMAGE analysis software. The area occupied by the infarct was measured as a percentage of the total LV area for four sections from each of five segments per sample, as done previously (24). Morphometry was used to determine cardiac myocyte size at infarct-remote zones (defined as the noninfarcted interventricular septum) by cross-sectional area measurements of myocytes in similar orientation and at the same magnification for all sections (29). Remote zone fibrosis was analyzed semiquantitatively by determination of the collagen volume fraction (15). Morphometry was performed by using NIH IMAGE analysis software. Ten random fields were assessed for each heart examined and mean values taken.

Hydroxyproline Assay by Chromatography. LV samples from 3 weeks were harvested and processed for hydroxyproline assay by HPLC, as previously done in our laboratory (30). Twenty microliters of tissue lysate (at 6 μg/μl) was hydrolyzed overnight with 500 μl of 6 M HCl at 105°C before loading onto HPLC columns.

Collagen and MMP Gene Expression. Total RNA was extracted from LVs by using TRIzol reagent (Invitrogen) according to the manufacturer's instructions. First-strand synthesis was performed with 1 μg of total RNA by using SuperScript II reverse transcriptase (RT; Invitrogen), as described (31). One microliter of the RT reaction product was used as cDNA template in subsequent PCR by using primers for the following genes: collagens proα1(I), α1(III); β-actin; transforming growth factor (TGF)β1; MMP-2; tissue inhibitor of MMP (TIMP)-1, -2 (sequences and conditions, Table 2). Ten microliters of each PCR product was run on 1.5% agarose gels and bands visualized with a UV transilluminator (Bio-Rad).

Gelatin Zymography. One hundred twenty micrograms of total protein lysate from LVs harvested at 1 and 3 weeks was used for loading onto 7.5% gelatin-polyacrylamide zymogram gels, as described (32). Supernatant from HT1080 human fibrosarcoma cells was used as positive control for MMP-2 and -9.

Statistical Analysis. All values are expressed as means ± SEM. Comparison among multiple groups was performed by one-way ANOVA followed by Bonferroni's post hoc test. A value of $P < 0.05$ was considered statistically significant. Statistical comparison of the data was performed by using the SIGMASTAT statistical package, Ver. 2.03 (SPSS, Chicago).

Results

***In Vitro* Characterization of sIL-1ra-Expressing SkM Clones.** *In vitro* expression of sIL-1ra was confirmed in cell lines by both enzyme immunoassay of cell culture supernatants and immunocytochemistry (ICC). The highest-expressing clone A4.20 (1207.6 pg/10^6 cells/24 h) was used in subsequent *in vivo* experiments, with clone B2.8 (no detectable sIL-1ra) as a control. ICC

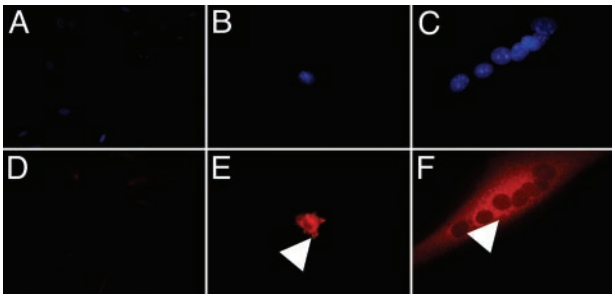

Fig. 1. Expression of sIL-1ra in *H-2K*^{b} clones. Immunocytochemistry demonstrates expression of sIL-1ra (red fluorescence) in a perinuclear distribution (within Golgi apparatus: arrows) in clone A4.20 SkM (*B* and *E*) and derived myotubes (*C* and *F*) after monensin treatment. In contrast, no clear staining is seen in the control cell line B2.8 (*A* and *D*). Nuclei stained with 4′,6-diamidino-2-phenylindole are shown in *A*–*C*.

confirmed expression of sIL-1ra in both undifferentiated A4.20 cells and myotubes with perinuclear accumulation in the Golgi apparatus after monensin treatment (Fig. 1). The proliferation rates and differentiation capacity of the *H-2K*^{b} cell lines generated were comparable with wild-type *H-2K*^{b} cells (data not shown).

Surgical Outcome, SkM Engraftment, and Human sIL-1ra Expression. Mortality over the 3-week period was: 26.9% (7/26), 29.6% (8/27), and 36.0% (9/25) for sIL-1ra-SkM, cont-SkM, and MI-only groups, respectively. The majority of deaths occurred within 48 h of MI. The standard curve generated from *smcy* PCR signals of known numbers of male SkM mixed with female control hearts (Fig. 2 *A* and *B*) was linear over the range tested ($R^2 = 0.95$). Greater numbers of donor-derived cells were found in the sIL-1ra-SkM group compared with cont-SkM (Fig. 2*C*) at both 1 (28 ± 3.7% vs. 20 ± 1.7%) and 3 weeks (17.8 ± 1.7% vs.2.7 ± 0.3%). RT-PCR using primers specific to the hsIL-1ra transgene yielded the expected product in samples at 3 weeks in only the sIL-1ra-SkM group (Fig. 2*D*). Specificity was confirmed by sequencing. No murine IL-1ra was seen (data not shown). Immunohistochemistry of sections from cell-engrafted hearts using skeletal fast myosin-specific antibody showed few myotube-like structures at infarct border zones in sIL-1ra-SkM-engrafted hearts at 3 weeks (Fig. 3). No clear evidence of myotube formation was seen in cont-SkM-engrafted hearts.

Effects of Cell Implantation on LV Function and Size. 2D and M-mode transthoracic echocardiographic images were obtained 3 weeks after MI and cell implantation (Fig. 4*A*). The highest systolic LV ejection fraction at 3 weeks was found in the sIL-1ra-SkM group (67.0 ± 2.3% compared with 55.7 ± 1.2% and 40.3 ± 2.9% for the cont-SkM and MI-only groups, respectively; Fig. 4*B*). These data compare with EF 71.3 ± 5.1% for noninfarcted untreated hearts. Only sIL-1ra-SkM-engrafted hearts showed significantly better preserved LVEDD at 3 weeks (sIL-1ra-SkM, 4.0 ± 1.1 mm; cont-SkM, 4.5 ± 1.2 mm; MI only, 4.8 ± 1.8 mm, Fig. 3*C*; normal untreated heart, 3.6 ± 0.2 mm). The E/A ratio was almost normalized in the sIL-1ra-SkM group (2.01 ± 0.25). The ratios in the cont-SkM and MI-only groups were reduced to 1.34 ± 0.10 and 1.16 ± 0.04, respectively; the E/A ratio differences between all groups were statistically different (Fig. 5). Comparison of percent lung/body weight showed a significant reduction in the sIL-1ra-SkM hearts compared with cont-SkM and MI-only hearts (Table 1.)

Changes in Cardiac Myocytes and ECM. Measurement of cardiac myocyte size in the remote zones revealed significantly less hypertrophy in sIL-1ra-SkM engrafted hearts compared with

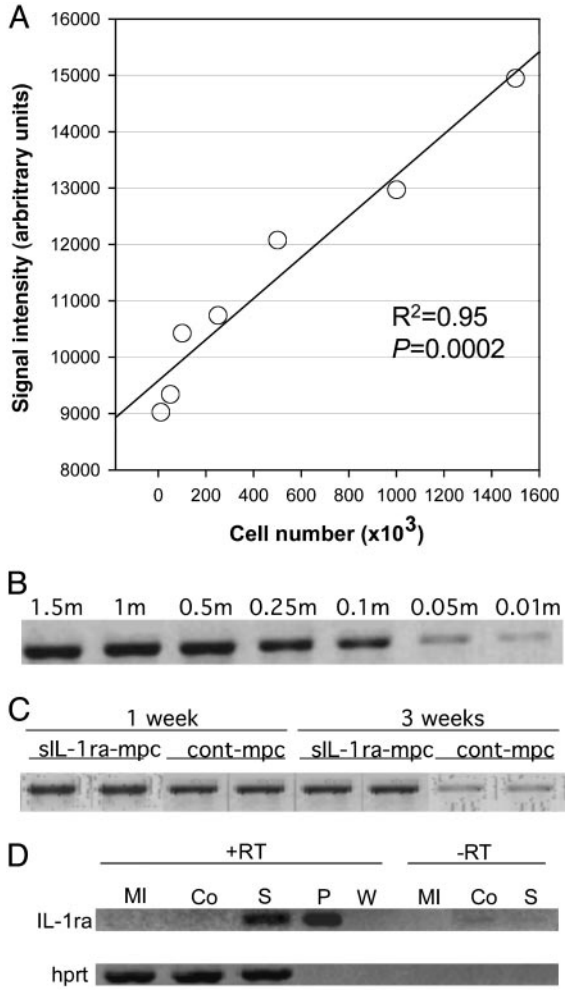

Fig. 2. *In vivo* persistence of *H-2K*^{b} clones and *in vivo* expression of sIL-1ra. Genomic *smcy* PCR was used to detect SkM at 1 and 3 weeks ($n = 4$ for each time point). A standard curve (*A*) was constructed in duplicate by using known numbers of cells [*B*; cell number in millions (m)]. Enhanced SkM numbers are suggested at both 1 and 3 weeks in the sIL-1ra-SkM group (*C*). (*D*) RT-PCR confirmed *in vivo* expression of sIL-1ra in sIL-1ra-SkM-engrafted hearts (S) at 3 weeks, although not in the cont-SkM (Co) or MI-only groups (MI). RT, reverse transcriptase; W, water; P, 10 ng pcDNA3.1$^+$-hsIL-1ra plasmid.

cont-SkM or MI-only hearts at 3 weeks (Fig. 6*A*). Lesser cardiac hypertrophy was also reflected in the s-IL-1ra-SkM hearts by a reduced percent LV/body weight ratio (Table 1). There were no significant differences in infarct size among groups (42.2 ± 7.2%, 47.5 ± 5.6%, and 47.3 ± 6.9% for sIL-1ra-SkM, cont-SkM, and MI-only groups, respectively). Picrosirius red staining revealed a marked reduction in total collagen accumulation in the sIL-1ra-SkM group in the remote noninfarcted septum at 3 weeks (Figs. 6*B* and 7*F*) and infarct border zones (Fig. 7*E*). Implantation of cont-SkM resulted in less collagen accumulation compared with MI-only hearts, although this was not significant (Fig. 6*B*). Hydroxyproline assay confirmed a significant reduction in collagen in the sIL-1ra-SkM group compared with the other groups at 3 weeks (0.58 ± 0.2, 0.68 ± 0.1, and 0.69 ± 0.1 μg of hydroxyproline per mg of tissue protein for sIL-1ra-SkM, cont-SkM, and MI-only hearts, respectively; $n = 4$, $P < 0.05$).

Changes in Collagen and MMP Expression. At 3 weeks, RT-PCR showed a clear reduction in pro α1col(I) expression in the sIL-1ra-SkM group compared with the MI-only and cont-SkM groups (Fig. 8). The levels of α1col(III) and TGFβ1 were similar

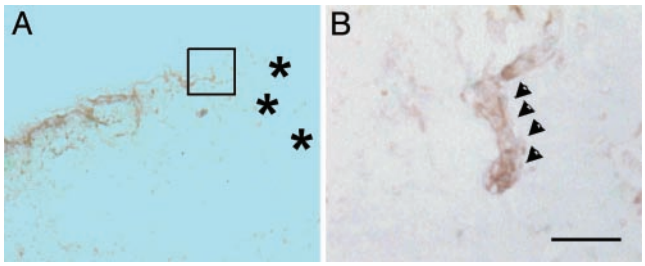

Fig. 3. Histological findings in sIL-1ra-SkM-engrafted hearts after 3 weeks using antibody specific for skeletal muscle fast myosin. (*A*) A small number of fast myosin+ve myotubes (horseradish peroxidase, brown) were observed at infarct border zones. (*B*) Serial section with higher-magnification view of myotube (arrowheads) within boxed region shown in *A*. No clear evidence of myotubes was found in cont-SkM-engrafted hearts. *, infarct. Counterstaining with methyl green. [Bar = 150 μm (*A*); 50 μm (*B*).]

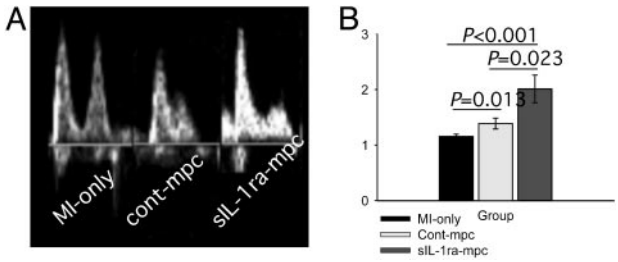

Fig. 5. LV diastolic function in infarcted hearts at 3 weeks. Diastolic transmitral E/A ratios were determined by measuring the height of peaks of flow through the mitral valve; representative echocardiographic spectral Doppler images are shown (*A*) SkM implantation had a significant beneficial effect on E/A ratio compared with nonengrafted infarcted hearts; this effect was greatest with sIL-1ra-SkM (*B*). All values mean ± SEM; $n = 5$ for each group.

in all groups (Fig. 8). Biochemical analysis of MMP-2 and -9 by gelatin zymography at 3 weeks showed their expression to be down-regulated in all groups (data not shown). We therefore obtained further samples at 1 week for zymography, because studies had shown that MMP-2 and -9 activity peak at 1–2 weeks post-MI in rodents even though mRNA levels remain elevated for 3 weeks (15, 33). We found a much lower expression of products corresponding to MMP-2 and -9 on zymography in both cell-engrafted groups compared with the MI-only group at 1 week (Fig. 9*A*). mRNA levels for MMP-2 were clearly reduced in the sIL-1ra-SkM hearts at 3 weeks by RT-PCR (Fig. 9*B*). There was also no apparent difference in expression of TIMP-1 or-2 (Fig. 9*C*).

Discussion

The data presented in this study show that SkM grafted to infarcted myocardium can induce changes in the cellular, biochemical, and molecular components of adverse remodeling, and that these changes may be significantly enhanced by targeting IL-1 as a key regulator of both the remodeling cascade and graft cell death.

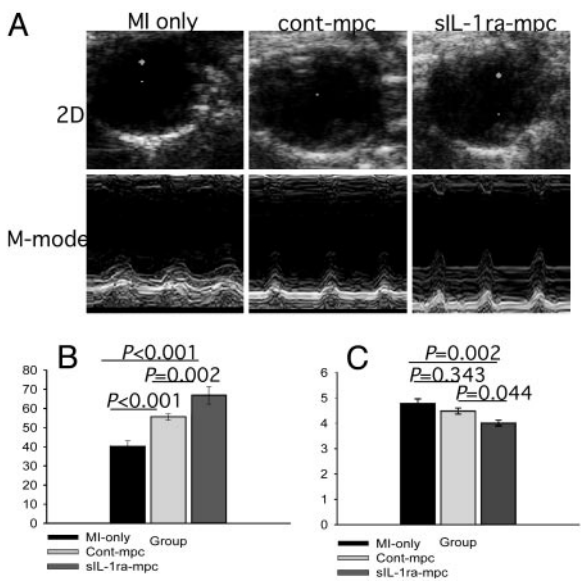

Fig. 4. LV function and size at 3 weeks. (*A*) Representative 2D (systole) and M-mode echocardiographic images are shown. (*B*) LV ejection fraction was significantly improved after implantation of either *H-2K*^{b} clone and was greatest with sIL-1ra-SkM. (*C*) There was a significantly lower LVEDD in hearts engrafted with sIL-1ra-SkM compared with cont-SkM and MI-only hearts, which did not differ significantly. All values are mean ± SEM; $n = 12$ for each group.

The improvement in systolic function seen in hearts engrafted with cont-SkM, compared with MI-only hearts, is consistent with previous studies (1, 2). LV ejection fraction was greatest after sIL-1ra-SkM implantation (67.0 ± 2.3%). This degree of functional improvement was unexpected given the size of the infarcts, although in keeping with the near normalization of LV systolic function post-MI reported by our own laboratory, using vascular endothelial growth factor-overexpressing SkM as grafts (24) and others using mesenchymal stem cells expressing the prosurvival *Akt* gene (34). It is possible that implanted SkM exert active contractile effects, as suggested by work on isolated strips of myocardium from SkM-engrafted hearts (35), although Leobon *et al.* (4) have recently suggested that SkM remain functionally isolated from host myocardium. One of the limitations of this study, however, is that serial echocardiography at time points shortly after infarction was not performed. This might help further clarify the mechanism of SkM effects.

LV dilatation post-MI is an important determinant of morbidity and mortality (5, 6) and was significantly attenuated in sIL-1ra-SkM-engrafted hearts at 3 weeks. Attenuated LV enlargement by SkM post-MI has been suggested by others (1). One could attribute this to a mechanical unloading effect of graft cells on LV wall stress, as seen with LV assist devices (36), although paracrine factors released by SkM/myotubes may also be important, and the effect of sIL-1ra-SkM is consistent with the correlation between IL-1 and LVEDD in infarcted rodent myocardium (8).

The improvement seen in diastolic E/A ratios after SkM grafting has been shown previously by us and others (1, 2, 24). Both cardiac hypertrophy and fibrosis are important determinants of diastolic dysfunction post-MI, although the exact relationships are not clear (5). We found a significant reduction in cardiac myocyte hypertrophy at infarct-remote zones after SkM implantation; this was further enhanced by SkM secreting IL-1ra, consistent with a role for IL-1 in cardiac hypertrophy (13). We

Table 1. LV- and lung-to-body weight ratios for infarcted hearts at 3 weeks

	Experimental group		
Ratio, %	sIL-lra-SkM	cont-SkM	MI only
LV/BWt	0.46 ± 0.04*†	0.61 ± 0.01	0.62 ± 0.01
Lung/BWt	0.93 ± 0.03*†	1.59 ± 0.12	1.88 ± 0.01

All values shown are mean ± SEM, $n = 4$. BWt, body weight. *, $P < 0.05$ vs. cont-SkM. †, $P < 0.05$ vs. MI only.

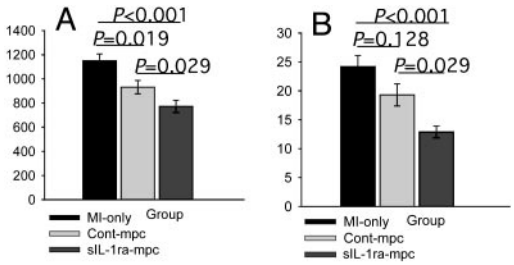

Fig. 6. Changes in remote-zone cardiac myocyte hypertrophy and fibrosis at 3 weeks. Cardiac myocyte size was determined by morphometry. There was a significantly lesser degree of hypertrophy in SkM-engrafted hearts compared with MI-only hearts; this was greatest after sIL-1ra-SkM implantation (*A*). Collagen volume fraction determination showed that only sIL-1ra-SkM implantation significantly attenuated fibrosis in infarcted hearts (*B*). All values are mean ± SEM; $n = 4$ for each group.

observed marked fibrosis in infarcted hearts, reflected in the collagen volume fraction and hydroxyproline content; this was significantly attenuated at infarct-remote zones by sIL-1ra-SkM although not by cont-SkM. One might expect a reduction in collagen accumulation to compromise the structural integrity of the myocardium (37). New collagen fibrils formed during the accelerated matrix turnover in experimental heart failure, however, are poorly crosslinked and structurally weak (38). Thus slowing the rapid cycle of collagen synthesis and degradation may be beneficial in attenuating both LV dilatation and diastolic dysfunction.

Pro α1col(I) transcription was decreased in the sIL-1ra-SkM group, although no clear difference was seen between cont-SkM and MI-only groups. Collagen type I is the most significant component of the ECM that accumulates post-MI (7, 8). No differences in col α1(III) or TGFβ1 expression were seen among groups. Although the difference in pro α1col(I) between the

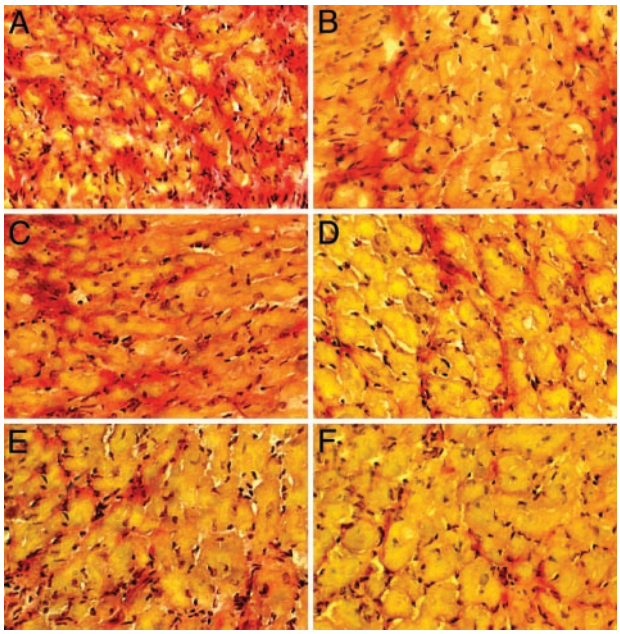

Fig. 7. Collagen accumulation in infarcted hearts at 3 weeks. Picrosirius red staining was used to highlight collagen (red) and myocytes (yellow) at infarct border (*A*, *C*, and *E*) and remote zones (*B*, *D*, and *F*). A reduced amount of collagen is apparent at the remote and infarct border zones in both cell-engrafted groups (sIL-1ra-SkM, *E*, *F*; cont-SkM, *C* and *D*) compared with the MI-only hearts (*A* and *B*) (×250).

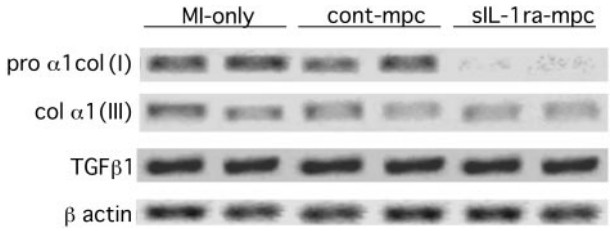

Fig. 8. Determination by RT-PCR of collagen I, III, and TGFβ1 expression at 3 weeks. There was a clear reduction in pro α1col(I) expression after sIL-1ra-SkM implantation, although not with cont-SkM, compared with MI-only hearts. In contrast, the levels of col α1(III) and TGFβ1 expression did not appear to differ between groups (β-actin expression is shown as an internal control).

sIL-1ra-SkM and other groups was clear, lesser differences among groups for the other genes cannot be excluded, and more quantitative analysis, such as by real-time PCR, would be needed to clarify this. The effects on pro α1col(I) seen in the sIL-1ra-SkM group may thus have occurred through a TGFβ1-independent pathway. Although IL-1β can enhance TGFβ1 expression, it can also directly induce transcription of col(I) (14, 39). A correlation between IL-1β and myocardial collagen content post-MI in rodents has been shown (8). In addition to changes in collagen expression, it was possible that SkM grafting and/or IL-1 inhibition had important effects on expression of genes relevant to matrix degradation.

MMP-2 and -9 were up-regulated on zymography at 1 week in the MI-only group, as observed by others (33). This up-regulation was significantly attenuated in both cell-engrafted groups. RT-PCR showed a clear decrease in MMP-2 in the sIL-1ra-SkM group at 3 weeks. Inhibition of MMPs after MI paradoxically results in less fibrosis, because collagen degradation products are potent inducers of matrix synthesis (9).

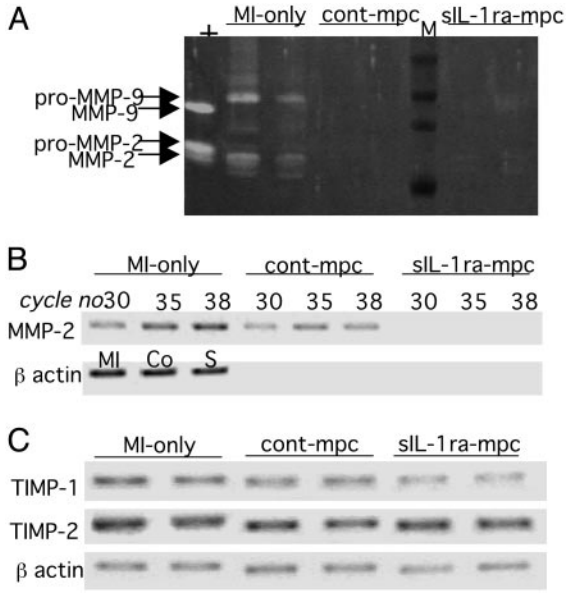

Fig. 9. Changes in MMP expression in infarcted hearts. (*A*) Gelatin zymography at 1 week shows reduced expression of products corresponding to MMP-2 and -9 in both cell-engrafted groups compared with MI-only hearts (+, HT1080 supernatant positive control; M, molecular weight markers). (*B*) At 3 weeks, decreased MMP-2 mRNA expression was evident only in the sIL-1ra-SkM-engrafted hearts, and a varying PCR cycle number showed that reactions were within saturation limits. (*C*) Expression of TIMP-1 and -2 was similar in all groups at 35 cycles. β-Actin internal controls are at 35 cycles in *B* (MI, MI-only; Co, cont-SkM; S, sIL-1ra-SkM) and *C*.

Whereas IL-1 is a potentially important upstream regulator of MMP-2 and -9 (16, 17), MMPs form a complex interacting network in the context of MI and are also subject to regulation by hypoxia and peptide growth factors; often through common regulatory elements such as AP-1 (16, 17). Interestingly, unloading the myocardium with an LV assist device in patients with ischemic cardiomyopathy results in decreased MMP-2 levels (40), and a similar effect after SkM implantation is a possibility. No apparent differences in TIMP-1 or -2 expression were found between groups, although more quantitative analysis would be needed to detect small changes in expression of these genes.

Importantly, graft size was significantly enhanced in our study using donor SkM expressing sIL-1ra compared with cont-SkM at both 1 (28 ± 3.7% vs. 20 ± 1.7%) and 3 weeks (17.8 ± 1.7% vs.2.7 ± 0.3%). These results are consistent with the involvement of IL-1 in acute-inflammatory-mediated graft cell death after grafting of SkM to muscle (12), proapoptotic effects of IL-1 on SkM *in vitro* (20), and the inhibitory effect of IL-1 on SkM proliferation (41). Graft loss is a major limitation of cell therapy, and strategies to attenuate environmental stress related to cytokines and free radicals may improve outcome, as we have observed (24, 42). Histological examination of engrafted hearts at 3 weeks showed very few donor-derived myotubes at infarct border zones in sIL-1ra-SkM-engrafted hearts. No clear myotubes were seen in cont-SkM-engrafted hearts, correlating with the much lower graft yield as determined by PCR for the *smcy* gene.

Taken together, these data suggest that paracrine factors play a major role in the mechanism of functional improvement seen after SkM grafting, as has recently been suggested by others (4). SkM expressing sIL-1ra exhibited greater graft cell numbers, although few resultant myotubes. This suggests that paracrine effects on adverse remodeling may have been relatively more important given evidence for the role of IL-1β in adverse remodeling. Consistent with this, we have previously shown beneficial effects of short-term IL-1ra expression on adverse remodeling within ischemia-reperfused rat hearts (10).

We conclude that SkM grafted to the border zones of infarcted myocardium can improve cardiac morphology and function through changes in the cellular, biochemical, and molecular components of adverse remodeling, and that these changes may be significantly enhanced by targeting IL-1 as a key regulator of both the remodeling cascade and graft cell death.

We thank Christine Marks and Kim Rogers (Siemens, U.K.) for expert assistance with echocardiography; and Hideaki Nagase and Linda Troeberg (Kennedy Institute of Rheumatology, Imperial College, London) for help with MMP zymography. This work was supported by the British Heart Foundation and Harefield Research Foundation. B.M. is a Research Training Fellow of the Medical Research Council, and K.S. is a Senior Clinical Fellow of the Medical Research Council.

1. Jain, M., DerSimonian, H., Brenner, D. A., Ngoy, S., Teller, P., Edge, A. S., Zawadzka, A., Wetzel, K., Sawyer, D. B., Colucci, W. S., *et al.* (2001) *Circulation* **103,** 1920–1927.
2. Taylor, D. A., Atkins, B. Z., Hungspreugs, P., Jones, T. R., Reedy, M. C., Hutcheson, K. A., Glower, D. D. & Kraus, W. E. (1998) *Nat. Med.* **4,** 929–933.
3. Koh, G. Y., Klug, M. G., Soonpaa, M. H. & Field, L. J. (1993) *J. Clin. Invest.* **92,** 1548–1554.
4. Leobon, B., Garcin, I., Menasche, P., Vilquin, J. T., Audinat, E. & Charpak, S. (2003) *Proc. Natl. Acad. Sci. USA* **100,** 7808–7811.
5. Pfeffer, J. M., Pfeffer, M. A., Fletcher, P. J. & Braunwald, E. (1991) *Am. J. Physiol.* **260,** H1406–H1414.
6. Pfeffer, M. A., Braunwald, E., Moye, L. A., Basta, L., Brown, E. J., Jr., Cuddy, T. E., Davis, B. R., Geltman, E. M., Goldman, S., Flaker, G. C., *et al.* (1992) *N. Engl. J. Med.* **327,** 669–677.
7. Cleutjens, J. P., Verluyten, M. J., Smiths, J. F. & Daemen, M. J. (1995) *Am. J. Pathol.* **147,** 325–338.
8. Ono, K., Matsumori, A., Shioi, T., Furukawa, Y. & Sasayama, S. (1998) *Circulation* **98,** 149–156.
9. Li, Y. Y., Feng, Y. Q., Kadokami, T., McTiernan, C. F., Draviam, R., Watkins, S. C. & Feldman, A. M. (2000) *Proc. Natl. Acad. Sci. USA* **97,** 12746–12751.
10. Suzuki, K., Murtuza, B., Smolenski, R. T., Sammut, I. A., Suzuki, N., Kaneda, Y. & Yacoub, M. H. (2001) *Circulation* **104,** I308–I313.
11. Yue, P., Massie, B. M., Simpson, P. C. & Long, C. S. (1998) *Am. J. Physiol.* **275,** H250–H258.
12. Qu, Z., Balkir, L., van Deutekom, J. C., Robbins, P. D., Pruchnic, R. & Huard, J. (1998) *J. Cell Biol.* **142,** 1257–1267.
13. Thaik, C. M., Calderone, A., Takahashi, N. & Colucci, W. S. (1995) *J. Clin. Invest.* **96,** 1093–1099.
14. Postlethwaite, A. E., Raghow, R., Stricklin, G. P., Poppleton, H., Seyer, J. M. & Kang, A. H. (1988) *J. Cell Biol.* **106,** 311–318.
15. Ducharme, A., Frantz, S., Aikawa, M., Rabkin, E., Lindsey, M., Rohde, L. E., Schoen, F. J., Kelly, R. A., Werb, Z., Libby, P., *et al.* (2000) *J. Clin. Invest.* **106,** 55–62.
16. Bergman, M. R., Cheng, S., Honbo, N., Piacentini, L., Karliner, J. S. & Lovett, D. H. (2003) *Biochem. J.* **369,** 485–496.
17. Creemers, E. E., Cleutjens, J. P., Smits, J. F. & Daemen, M. J. (2001) *Circ. Res.* **89,** 201–210.
18. Zhang, M., Methot, D., Poppa, V., Fujio, Y., Walsh, K. & Murry, C. E. (2001) *J. Mol. Cell Cardiol.* **33,** 907–921.
19. Guerette, B., Skuk, D., Celestin, F., Huard, C., Tardif, F., Asselin, I., Roy, B., Goulet, M., Roy, R., Entman, M., *et al.* (1997) *J. Immunol.* **159,** 2522–2531.
20. Authier, F. J., Chazaud, B., Plonquet, A., Eliezer-Vanerot, M. C., Poron, F., Belec, L., Barlovatz-Meimon, G. & Gherardi, R. K. (1999) *Cell Death Differ.* **6,** 1012–1021.
21. Eisenberg, S. P., Brewer, M. T., Verderber, E., Heimdal, P., Brandhuber, B. J. & Thompson, R. C. (1991) *Proc. Natl. Acad. Sci. USA* **88,** 5232–5236.
22. Morgan, J. E., Beauchamp, J. R., Pagel, C. N., Peckham, M., Ataliotis, P., Jat, P. S., Noble, M. D., Farmer, K. & Partridge, T. A. (1994) *Dev. Biol.* **162,** 486–498.
23. Springer, M. L., Chen, A. S., Kraft, P. E., Bednarski, M. & Blau, H. M. (1998) *Mol. Cell* **2,** 549–558.
24. Suzuki, K., Murtuza, B., Smolenski, R. T., Sammut, I. A., Suzuki, N., Kaneda, Y. & Yacoub, M. H. (2001) *Circulation* **104,** I207–I212.
25. Yang, X. P., Liu, Y. H., Rhaleb, N. E., Kurihara, N., Kim, H. E. & Carretero, O. A. (1999) *Am. J. Physiol.* **277,** H1967–H1974.
26. Beauchamp, J. R., Morgan, J. E., Pagel, C. N. & Partridge, T. A. (1999) *J. Cell Biol.* **144,** 1113–1122.
27. Agulnik, A. I., Longepied, G., Ty, M. T., Bishop, C. E. & Mitchell, M. (1999) *Mamm. Genome* **10,** 926–929.
28. Lu, Q. L., Morris, G. E., Wilton, S. D., Ly, T., Artem'yeva, O. V., Strong, P. & Partridge, T. A. (2000) *J. Cell Biol.* **148,** 985–996.
29. Passier, R., Zeng, H., Frey, N., Naya, F. J., Nicol, R. L., McKinsey, T. A., Overbeek, P., Richardson, J. A., Grant, S. R. & Olson, E. N. (2000) *J. Clin. Invest.* **105,** 1395–1406.
30. Wong, K., Boheler, K. R., Petrou, M. & Yacoub, M. H. (1997) *Circulation* **96,** 2239–2246.
31. Beauchamp, J. R., Heslop, L., Yu, D. S., Tajbakhsh, S., Kelly, R. G., Wernig, A., Buckingham, M. E., Partridge, T. A. & Zammit, P. S. (2000) *J. Cell Biol.* **151,** 1221–1234.
32. Morodomi, T., Ogata, Y., Sasaguri, Y., Morimatsu, M. & Nagase, H. (1992) *Biochem. J.* **285,** 603–611.
33. Peterson, J. T., Li, H., Dillon, L. & Bryant, J. W. (2000) *Cardiovasc. Res.* **46,** 307–315.
34. Mangi, A. A., Noiseux, N., Kong, D., He, H., Rezvani, M., Ingwall, J. S. & Dzau, V. J. (2003) *Nat. Med.* **9,** 1195–2001.
35. Murry, C. E., Wiseman, R. W., Schwartz, S. M. & Hauschka, S. D. (1996) *J. Clin. Invest.* **98,** 2512–2523.
36. Yacoub, M. H. (2001) *Eur. Heart J.* **22,** 534–540.
37. McCormick, R. J., Musch, T. I., Bergman, B. C. & Thomas, D. P. (1994) *Am. J. Physiol.* **266,** H354–H359.
38. Woodiwiss, A. J., Tsotetsi, O. J., Sprott, S., Lancaster, E. J., Mela, T., Chung, E. S., Meyer, T. E. & Norton, G. R. (2001) *Circulation* **103,** 155–160.
39. Vesey, D. A., Cheung, C., Cuttle, L., Endre, Z., Gobe, G. & Johnson, D. W. (2002) *J. Lab. Clin. Med.* **140,** 342–350.
40. Li, Y. Y., Feng, Y., McTiernan, C. F., Pei, W., Moravec, C. S., Wang, P., Rosenblum, W., Kormos, R. L. & Feldman, A. M. (2001) *Circulation* **104,** 1147–1152.
41. Ji, S. Q., Neustrom, S., Willis, G. M. & Spurlock, M. E. (1998) *J. Interferon Cytokine Res.* **18,** 879–888.
42. Suzuki, K., Smolenski, R. T., Jayakumar, J., Murtuza, B., Brand, N. J. & Yacoub, M. H. (2000) *Circulation* **102,** III216–III221.